JOURNAL OF PROPULSION AND POWER
Vol. 24, No. 5, September–October 2008

Chemi-Ion-Current-Induced Dissociative Recombination in Premixed Hydrocarbon/Air Flames

David L. Wisman*
UES, Inc., Dayton, Ohio 45432
S. D. Marcum†
Miami University, Oxford, Ohio 45056
and
Biswa N. Ganguly‡
Air Force Research Laboratory, Wright–Patterson Air Force Base, Ohio 45433

DOI: 10.2514/1.31823

This work focuses on the effects of a chemi-ion current induced by an applied positive bias on downward propagating, atmospheric pressure premixed hydrocarbon-air flames fueled by methane (CH_4), propane (C_3H_8), and *n* butane (C_4H_{10}). Applied voltages up to 3.2 kV over a 40 mm gap encompassing the flame front have been used to observe flame height and stability modifications compared with the no-applied-voltage case in flames with equivalence ratios of 1.0 and flow velocities up to 1.3 m/s. The observed experimental results suggest that, under the conditions studied for this work, the ionic wind is not responsible for the flame modifications. Chemi-ion-current-driven flame ion recombination chemistry that would produce light reactants near the burner head, similar to externally sustained plasma-assisted combustion techniques, is proposed to account for the observed flame perturbations. Current-continuity-based calculations that allow estimates of the production level for these reactants are reported. Possible flame fluid and flame chemistry modifications caused by the production of light radicals are also discussed.

I. Introduction

THE effects of applying an electric field on a flame have been studied since the early 1800s [1] when Brande noticed an effect on the heat and mass transfer of a diffusion flame between electrodes, which was then later verified in 1931 by Lewis [2]. During the late 1950s through the 1960s, the first detailed investigations of electric fields on flames were performed, and the causes of the observed effects were attributed to the ionic wind [3,4]. Those researchers proceeded to calculate theoretical maxima for the measured current densities in the flame as well as the ionic wind body-force-induced pressure changes [3].

As we reported previously, for premixed propane/air flames [5,6] we observe changes in the flame structure and flame height at applied voltages too small to be explained by the ionic wind theory. Therefore, we have recently proposed the dissociative recombination of positive flame ions [6] with electrons on the cathode surface leading to the production of light, highly diffusive radicals as an alternative explanation for the observed effects.

It is widely known [7–10] that the observed stability in a premixed flame is actually due to the competition between three different flame instabilities: hydrodynamic, thermodiffusive, and body force. The hydrodynamic instability is a fluid mechanical effect that was originally discovered independently by Darrieus [11] in 1938 and Landau [12] in 1944. It is caused by the thermal expansion of gases at the flame front, which leads to a temperature gradient that deviates the flow lines from the normal, causing a wrinkling [13], and is dominant under conditions of high flow speed. The thermodiffusive instability is caused by a preferential diffusion of molecular species vs heat in the immediate vicinity of the flame front and is highly dependent on the Lewis number of the deficient light reactant in the flame [7]. This instability is typically associated with flames near the flammability limits ($\phi < 0.8$ and $\phi > 1.4$). The naturally occurring body-force instability that is inherent to a flame arises because the burned and unburned gases have different densities and is similar to the Rayleigh–Taylor instability associated with fluids [8]. As shown by previous studies [9], the thermodiffusive instability has a strong dependence on the Lewis number (Le) of the flame, and lowering it can cause the flame surface to become wrinkled and unstable (Le is the ratio of the thermal diffusivity to the mass diffusivity). The production of light radicals from the dissociative recombination process [6] in the preheat zone of the flame may be sufficient to modify the thermodiffusive properties of the flame and lower the local Le.

In this paper, we present calculations of the ionic-wind-induced volumetric body-force and pressure changes at the experimental conditions discussed and investigate how the issue of flame stability applies to the ionic wind and the observed results. Additionally, we extend the previously reported results for propane/air flames to other premixed hydrocarbon flames, in particular methane/air and butane/air flames. The comparison of these three fuels allows us to investigate the effects of fuel properties, such as fuel Lewis number and chemi-ionization chemistry, on the observed results.

II. Experimental Setup

The principal setup, shown in Fig. 1, has been discussed in detail elsewhere [5,6]. The dc current-voltage (I/V) characteristics shown in Fig. 2 were recorded with the burner grounded and a positive bias (up to 3.2 kV) supplied to the upper disk electrode. As we reported previously [5], the use of a positive applied bias to the flame is critical for the observed results; when a negative polarity bias is applied, the current passing through the flame is negligible and there is no observable effect on the flame. These I/V measurements were made to gauge the coupling between the electric field and the flame and to investigate how the flame conductivity varied as a function of fuel. The electrode discussed is a 5-cm-diam stainless steel disk that was perforated in a honeycomb pattern with 44 3.2 mm holes, and was

Received 27 April 2007; revision received 30 January 2008; accepted for publication 23 May 2008.

*Research Scientist, Power and Propulsion Division. Member AIAA.
†Associate Professor, Department of Physics. Member AIAA.
‡Research Physicist, Propulsion Directorate. Associate Fellow AIAA.

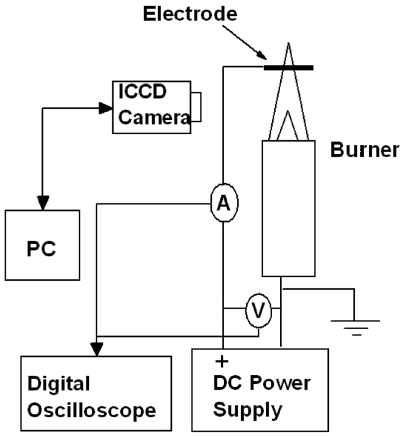

Fig. 1 Experimental setup for electric-field-induced flame modification experiment.

suspended 40 mm above the grounded burner. This allowed for a parallel-plate-like electrode geometry at the expense of perturbing the gas flow downstream from the flame front. The voltage is applied to the flame through a 500 kΩ current limiting ballast resistor that was connected between the anode and the dc bias supply for safety reasons, whereas the current measurements were made by measuring the voltage drop across a 100 kΩ current sense resistor.

Spectrally resolved images (Figs. 3–5) used to document the response of the flame to the applied voltage were obtained using a Princeton Instruments intensified charge coupled device (ICCD) high-speed camera and a 308 nm interference filter. The blurring of the flame front seen with an applied voltage is caused by the long time exposure (10 ms) and the strong unstable motion of the flame front. Broadband imaging was also taken at short exposure times (200 μs) to capture the time-resolved motion of the flame with applied voltage.

Gas temperature measurements at the burner head were made using an Omega infrared pyrometer, which was corrected for the emissivity of the cathode metal. These temperature measurements indicate a gas temperature near the cathode surface (preheat zone) of approximately 800 K. Under conditions with a low reduced electric field (E/n), it is reasonable to assume that the gas temperature and electron temperature are roughly equal, an approximation that will be used in our radical number density calculations. Estimations of the area of current collection were made by multiplying the circumference of the conical flame base by the thickness of the chemi-ionization region. Using previously reported results by MacLatchy [14], we estimate the thickness of the chemi-ionization region to be 0.15 cm, which gives a current collection area of 0.70 cm^2, for our burner.

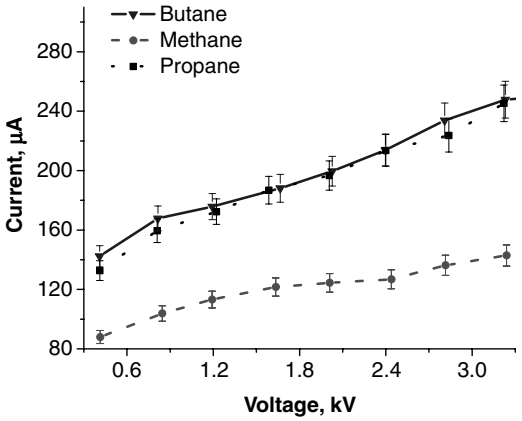

Fig. 2 Current and voltage characteristics for premixed flames fueled by methane, propane, and butane. The flame was at atmospheric pressure with an equivalence ratio of 1.0 and a flow speed of 1.3 m/s.

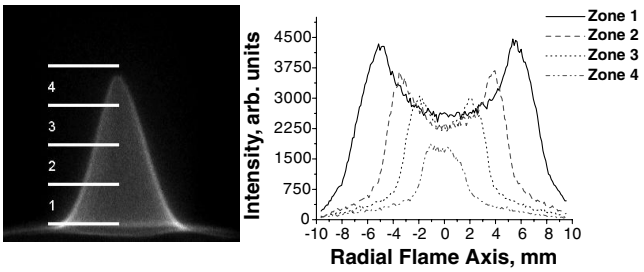

a)

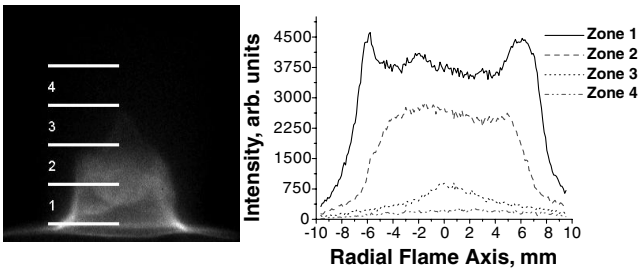

b)

Fig. 3 Spectrally resolved images of a methane flame at atmospheric pressure with an equivalence ratio of 1.0: a) no applied voltage, and b) 3.2 kV applied voltage. Zone intensities are plotted to the left as a function of the radial flame axis for both figure parts.

III. Theoretical Background

A. Ionic Wind Theory

As mentioned earlier, the ionic wind theory has been used by other researchers [3,4] to explain the effects of electric fields on flames. The ionic wind body force arises from ion–molecule and electron–molecule elastic scattering collisions. Expressions for the ion- and electron-induced forces per unit volume are indicated as follows [15]:

$$f_i = n_i m_i \nu_{\text{im}} u_i \tag{1a}$$

$$f_e = n_e m_e \nu_{\text{em}} u_e \tag{1b}$$

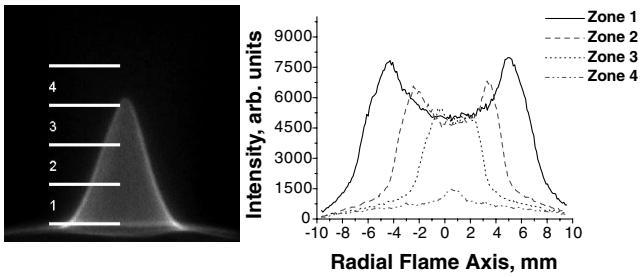

a)

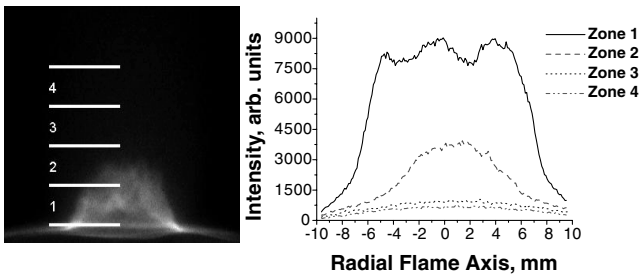

b)

Fig. 4 Spectrally resolved images of a propane flame at atmospheric pressure with an equivalence ratio of 1.0: a) no applied voltage, and b) 3.2 kV applied voltage. Zone intensities are plotted to the left as a function of the radial flame axis for both figure parts.

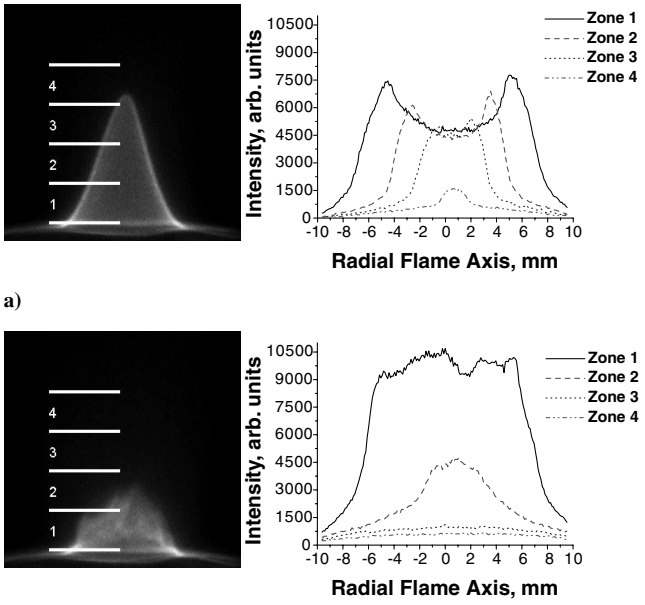

Fig. 5 Spectrally resolved images of a butane flame at atmospheric pressure with an equivalence ratio of 1.0: a) no applied voltage, and b) 3.2 kV applied voltage. Zone intensities are plotted to the left as a function of the radial flame axis for both figure parts.

where n is the number density, m is the mass, ν is the collision frequency, and u is the velocity. The subscripts i and e refer to ion and electron, respectively. Following the steps outlined by Boeuf and Pitchford [15], we can combine and rewrite Eqs. (1a) and (1b) in terms of the mobility, μ, and the current density, j, that is,

$$f = \left(\frac{j_i}{\mu_+} - \frac{j_e}{\mu_-}\right) \tag{2}$$

Using the current densities defined by the drift-diffusion equations, $j_i = en_i\mu_i E - eD_i\nabla n_i$, $j_e = en_e\mu_e E - eD_e\nabla n_e$, we can write the force per unit volume as

$$f = e(n_i - n_e)E - kT_i\nabla n_i - kT_e\nabla n_e \tag{3}$$

where e is the fundamental charge, E is the electric field, k is Boltzmann's constant, and T_i and T_e are the ion and electron temperatures, respectively.

With the experimental setup discussed in this paper, the only location in the flame at which there is a charge separation ($n_i \neq n_e$) is at the burner head, where a cathode sheath forms. As will be shown through the calculations in Sec. IV of this paper, the contribution to the total force from the gradient terms of Eq. (3) is small compared with the first term; thus, the gradient term contributions can be neglected in our case. Because a cathode sheath forms, the number density of positive ions at the sheath will far exceed that of electrons. These approximations allow us to rewrite Eq. (3) as

$$f = Een_i \tag{4}$$

It is important to remember that Eq. (4) is a volumetric force; therefore, multiplying it by a spatial variable (the thickness of the sheath) gives the induced pressure change. For these results, the thickness of the sheath was taken to be 5 electron Debye lengths, where the Debye length can be written [16] as $\lambda_D = 742(\frac{T[\mathrm{eV}]}{n_e})^{1/2}$. Using this sheath thickness and expression for the force in Eq. (4), we arrive at the following expression for the ionic-wind-induced pressure change across the flame:

$$\Delta p = 5Een_i\lambda_D \tag{5}$$

Any observable effect of the ionic wind body force on the flame should be distributed across the flame, and under conditions of a positive applied bias the body force would cause a general downward acceleration of the flame [17]. For the flame conditions in this paper, for which there is a downward propagating flame, these ionic wind body forces would act to aid the inherent gravitational body forces and lead to an increase in the flame stability [8].

B. Radical Production

Experimental studies have shown that the ionic species in methane/air [18,19] and propane/air [20] flames are similar and, because butane chemistry is similar to that of propane, we can extend this similarity to butane as well. Although the three fuels give rise to similar ionic species, all derived from the chemi-ionization processes, they have slightly different levels of chemi-ions produced when burned. This result is evident when looking at the I/V curves in Fig. 2. The aforementioned experimental results [18–20] indicate that in the downstream burned-gas region of the flame the primary ionic species are H_3O^+, NO^+, and HCO^+, accounting for approximately 90, 7, and 3% of the overall ionic population, respectively. Using this ionic species information, we can write the following current continuity relation:

$$n_{H_3O^+} \cdot v_{d,H_3O^+} + n_{HCO^+} \cdot v_{d,HCO^+} + n_{NO^+} \cdot v_{d,NO^+} + n_e \cdot v_{d,e} = j/e \tag{6}$$

where v_d is the drift velocity.

In the cathode sheath region, the number density of electrons will approach zero; thus, the electron current conduction term can be neglected in the calculations of Eq. (6). Also, as the positive flame ions approach the cathode, the Bohm criterion states that they will be accelerated from their normal drift velocities to their ionic Bohm velocities, which can be expressed [21] as $v_B = (\frac{kT_e}{m_{\mathrm{ion}}})^{1/2}$. Using this information with the aforementioned percentages of total ion concentration, and expanding the current density as the measured current, I, divided by the area over which this current is collected, A, we can rewrite Eq. (6) as

$$0.9n_{\mathrm{ion}} \cdot \left(\frac{kT_e}{m_{H_3O^+}}\right)^{1/2} + 0.7n_{\mathrm{ion}} \cdot \left(\frac{kT_e}{m_{NO^+}}\right)^{1/2} + 0.3n_{\mathrm{ion}} \cdot \left(\frac{kT_e}{m_{HCO^+}}\right)^{1/2} = \frac{I}{A \cdot e} \tag{7}$$

To calculate the radical number densities from the ion number densities, we need to know the recombination chemistry of each of the aforementioned ions. The NO^+ ion recombines via $NO^+ + e^- \rightarrow NO$, whereas H_3O^+ and HCO^+ dissociatively recombine. The dissociation channels for H_3O^+ are listed below [22], whereas HCO^+ only dissociates via $HCO^+ + e^- \rightarrow H + CO$.

$$H_3O^+ + e^- \Rightarrow \begin{cases} H_2O + H, N = 0.05 \\ OH + H_2, N = 0.36 \\ OH + 2H, N = 0.29 \\ O + H + H_2, N = 0.30 \end{cases}$$

The numbers to the right of the dissociation branches indicate the probability that H_3O^+ will dissociate by means of that particular channel. Multiplying these probabilities by the radicals for each of the dissociation branches, and weighting by the ion number densities calculated from Eq. (7), allows an estimation of the number density of light radicals produced at the cathode surface.

IV. Results and Discussion

As seen in Fig. 2, the conductivities in the propane and butane flames are similar, whereas the conductivity of the methane flame is lower than the other flames. These differences in conductivity are attributed to the different chemical properties of the fuels, which cause different amounts of chemi-ionization-derived ions to be produced. For the data presented in Fig. 2, the flow speed was kept constant at 1.3 m/s and the equivalence ratio was 1.0 for all three flames.

In Figs. 3–5, we can see the effects of the applied positive bias on each flame. Figure 3a is a methane/air flame with no applied voltage, whereas Fig. 3b is the same methane flame but with an applied voltage of 3.2 kV. As seen from the indicated lines, the flame in both images was divided into four zones of equal image area (labeled 1–4). The intensity profiles to the right of the images indicate the grayscale intensity values of the image as a function of the radial flame axis. The zones in Figs. 3a and 3b are at the same pixel locations; thus, by comparing the intensity profiles in Figs. 3a and 3b, it is possible to see how the location of the intensity varies with the applied voltage. The images in Fig. 3 were taken with the use of a 308 nm bandpass filter to allow the imaging of the OH^* chemiluminescence signals of the flame. The main source of the OH^* in the flame comes from the reaction [23] $CH + O_2 \rightarrow OH^* + CO$ and, therefore, has been shown to be useful as a marker for the flame front [24], as well as for the location of the heat release in the flame [25,26]. Similar results to those discussed for Fig. 3 can be seen for propane (Fig. 4) and butane (Fig. 5).

The results of the intensity plots in Figs. 3–5 show that, as the voltage is applied to the flame, the heat release of the flame is confined to a smaller volume (the intensity from zones 3 and 4 are added to zones 1 and 2). This can also be seen by looking at the images in those figures; as we apply the voltage to the flame, the flame height is decreased. Comparing the change in flame height in Figs. 3a, 3b, 4a, 4b, 5a, and 5b, we see a similar change in flame height of approximately 60% for propane and butane and a change in flame height of approximately 50% for methane. By measuring the total integrated intensity (which is both time averaged and volume averaged) of the images, we find that there is no significant modification to the amount of heat release. This, coupled with the aforementioned observation of a shorter flame, indicates that with all three fuels we see an increase in the combustion intensity near the burner head as we apply a positive voltage in the downstream region of the flame.

The choice of these three particular fuels also allowed us to investigate the effect of fuel Le on the observed results. Under stoichiometric conditions, methane/air flames have an Le of approximately 1.1, whereas propane/air and butane air have an Le of approximately 1.9 and 2.1, respectively [27]. These differences in fuel Le could potentially have implications with regard to the flame stability issues. Figure 6 shows a set of images of a propane/air flame at four different applied voltages. These images were taken under broadband conditions to allow the capture of time-resolved (200 μs exposure) flame structure changes at various applied voltages. These images show that, as the positive bias on the flame is increased, the flame structure becomes more wrinkled and unstable. This unstable motion of the flame is also inferred from the blurring in the time-averaged flame images in Figs. 3–5, indicating that all three fuels transition from a similar quasi-laminar flame structure to an *unstable* flame structure with the application of a positive bias on the flame.

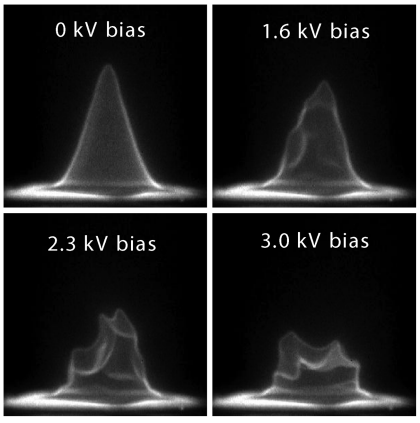

Fig. 6 Broadband images of a propane flame at atmospheric pressure with an equivalence ratio of 1.0. Starting from left to right the voltage is increased (as indicated above the flame) to show time-resolved flame structure changes with an applied voltage.

In Sec. III, we discussed two potential explanations for the experimental results. The total volumetric body force on the flame due to the ionic wind can be calculated using Eq. (4) if we neglect the contribution from the gradient terms of Eq. (3). If we use an average number density of positive ions for the three fuels of 3×10^{16} m^{-3}, calculated using Eq. (7), and assume a maximum possible gradient over a distance of 1 mm (a few times the flame thickness at atmospheric pressure [28]) at a flame temperature of 2000 K, we calculate that the gradient terms give a contribution of $f_{\text{grad}} = 0.7$ N/m^3. To calculate the volume force term from the ionic wind at the sheath, we first need to calculate the electric field value at the sheath using Poisson's equation:

$$\int_{E_o}^{E_s} \mathrm{d}E = 4\pi n_i e \int_0^{\delta_s} \mathrm{d}x \tag{8}$$

where E_o is the volume-averaged electric field found by measuring the voltage drop over certain distance in the flame (with a lower bound value measured to be $\sim 5 \times 10^4$ V/m), δ_s is the sheath thickness, taken to be 5 electron Debye lengths, and E_s is the average value of the electric field in the sheath. Using the aforementioned values, we find an approximate E_s of 1×10^5 V/m, which then gives a value of the force term at the sheath of 500 N/m^3. As can easily be seen comparing the total force contributions from the gradient terms and the sheath terms, the gradient terms are much smaller and thus can be neglected. If we multiply the value of the volumetric force, already calculated, by the sheath thickness, δ_s, we arrive at a value for the pressure change in the preheat zone due to the ionic wind of 0.03 Pa.

The pressure changes calculated herein are too small to account for the flame front modifications observed in Figs. 3–5. Additionally, as mentioned in Sec. I, under conditions of a downward propagating flame the body-force effect from the downward oriented electric force should have a stabilizing effect on the flame [8], but as shown in the flame images already discussed, there is a destabilizing effect on the flame. It was also mentioned that the effects of the ionic wind body force should be distributed along the flame and cause a downward acceleration [17]; however, the flame images in Fig. 7 indicate otherwise. The initial modification of the flame under these conditions is a constriction of the base of the flame, which then moves radially inward leading to an eventual flame pinch off, as seen

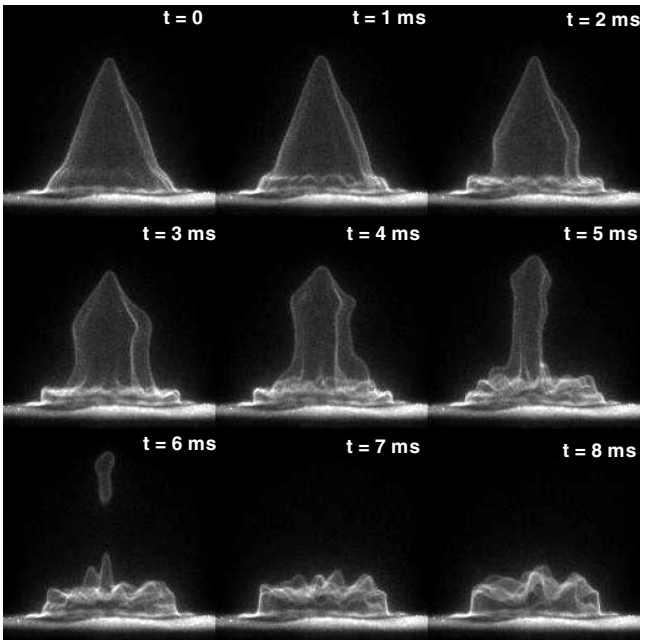

Fig. 7 High-speed images (100 μs exposures) of a propane/air flame ($\phi = 1.1$) response to a positive pulsed bias of 4.0 kV. This set of images indicates that the modification to the flame begins with a constriction at the base of the flame that moves upward and eventually leads to a pinch off, giving the highly unstable flame structure seen at the later times.

Table 1 Radical number densities for methane, propane, and butane that are produced from the chemi-ion-current-induced dissociative recombination of positive flame ions in the preheat zone

	Methane, cm^{-3}	Propane and butane, cm^{-3}
n_H	2×10^{10}	3×10^{10}
n_{OH}	1×10^{10}	2×10^{10}
n_O	3×10^{9}	1×10^{10}
n_{H_2}	1×10^{10}	2×10^{10}
n_{CO}	7×10^{8}	1×10^{9}
n_{H_2O}	1×10^{9}	2×10^{9}
n_{NO}	2×10^{9}	3×10^{9}

at $t = 6$ ms in Fig. 7. These high-speed flame images (100 μs exposures) were taken with a positive pulsed bias of 4.0 kV being applied to the flame and are similar to results reported previously [5]. This pocket formation (pinch off) is an additional indication that the flame has become highly unstable and is similar to flames with an Le below unity (thermodiffusive dominated) [29]. The origination of this flame modification at the base of the flame, as well as the transition to an unstable flame (with all three fuels), are both counter to the effects that should occur with the ionic-wind-induced body force for a downward propagating flame. This information, along with the small pressure changes calculated using Eq. (5), suggests that under the experimental conditions discussed in this paper (low applied voltage) the ionic wind is not responsible for the observed changes.

As an alternative explanation, we proposed the recombination of flame ions as a plausible cause for the observed changes. Using Eq. (7), as well as the maximum measured currents for each of the fuels (found in Fig. 2), we calculate the approximate number densities of radicals produced in the preheat zone of the flame by recombination and present those results in Table 1. Because propane and butane had similar conductivities, they will have similar amounts of radicals produced and are therefore listed in the same column. It is important to note that these radicals are being produced in the preheat zone and, at this location, the gas temperature is low (800 K), implying that the preexisting radical number densities from combustion processes are smaller than the radicals produced through the recombination of the chemi-ion current [30]. These radicals produced in the preheat zone of the flame are light and highly diffusive, and an increase in the concentration of light, highly diffusive reactants could cause the local flame Le to drop to values below unity. This modification of the Le could change the thermodiffusive properties of the flame [31], which could lead to a wrinkled, unstable flame structure, consistent with the results seen in Fig. 6 [9,31]. These results also show trends similar to dielectric barrier discharge (DBD) plasma-assisted combustion results, in which radicals are injected near the base of the flame [32–34]. Typical input powers of the DBD experiments vary but, in some cases [33], are nearly identical to our input power.

In addition to the fluidic changes discussed, the flame kinetics can be modified by the production of these radicals as well. The effect of such kinetic modifications can be seen in the time-resolved, volume-averaged OH* intensity plot in Fig. 8. In this figure, we see a delayed increase in the OH* intensity of approximately 15%, which peaks after the termination of the voltage pulse. The OH* data presented in this figure were obtained with a positive pulsed bias of approximately 2.4 kV applied to the flame and by imaging the entire flame onto a photomultiplier tube (PMT) with a 308 nm bandpass filter (the PMT bias was negative, and so a negative signal indicates an increase in emission intensity). The pulsed data in Fig. 8 indicate that there is approximately 0.6 W of time-averaged power per pulse, using a 30% duty cycle, whereas for the dc data in Fig. 2, we had an input power of approximately 0.8 W. Both cases represent similar input powers (the average power in the pulsed data will be less due to the low duty cycle), indicating there will be similar amounts of energy input and thus allowing us to compare the results of the two cases. This *time-resolved* OH* data indicate that there is a slight increase of the total heat release (which was not seen in the *time-averaged* images in Figs. 3–5) of the flame with the applied voltage and that it peaks *after* the voltage pulse has ended, which is an indication that chemi-ion-current-induced radical production in the preheat zone enhances flame kinetics and global heat release.

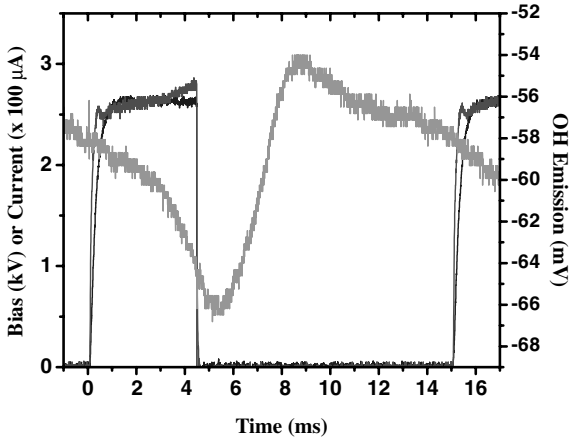

Fig. 8 Current, bias voltage, and total OH* emission intensity for a 4.2 ms pulsed bias of a premixed propane/air flame at an equivalence ratio of 1.1. Note that the OH* chemiluminescence signal increases by approximately 15% and peaks *after* the voltage pulse has been terminated.

V. Conclusions

In this work, we have investigated the effect of both dc and pulsed applied positive bias on flames fueled by methane, propane, and butane. The results presented show that all three flames have similar changes in flame height with the same applied bias, irrespective of the fuel Lewis number. The magnitude of the effect on the flame is strongly dependent on the level of chemi-ion current measured at the cathode. Methane, having the smallest measured chemi-ion current, has a slightly smaller change in flame height (than propane and butane) with the applied bias, whereas both propane and butane, having similar measured chemi-ion currents, have similar changes in flame height that are slightly greater than that of methane. The small calculated ionic wind body-force-induced pressure changes, as well as the observations that the flame disturbance originates at the base of the flame and the applied voltage has a destabilizing effect, together suggest that the ionic wind is not responsible for the observed effects on the flame under the low applied voltage conditions studied in this paper. Therefore, we have investigated the alternative explanation of the production of light radicals through a chemi-ion-current-induced recombination of positive flame ions with electrons on the cathode surface. The number densities of the radicals produced from this process were estimated, and a plausible mechanism was offered as to the importance of the location at which these radicals were produced, which may modify the flame fluidics (lowering of the Le) and flame kinetic changes, as evident by the modulation of the heat release of the flame observed in the time-resolved PMT signal.

Acknowledgments

This work was supported in part by the Air Force Office of Scientific Research (AFOSR), Julian Tishkoff, technical monitor. S. D. Marcum thanks the U.S. Air Force Summer Faculty Fellowship Program (SFFP) for partial funding. All work was performed at Wright-Patterson Air Force Base, Ohio.

References

[1] Fialkov, A., "Investigations on Ions in Flames," *Progress in Energy and Combustion Science*, Vol. 23, Nos. 5–6, 1997, pp. 399–528. doi:10.1016/S0360-1285(97)00016-6

[2] Lewis, B., "The Effect of an Electric Field on Flames and Their Propagation," *Journal of the American Chemical Society*, Vol. 53, No. 4, 1931, pp. 1304–1313. doi:10.1021/ja01355a018

[3] Lawton, J., and Weinberg, F., "Maximum Ion Currents from Flames

and the Maximum Practical Effects of Applied Electric Fields," *Proceedings of the Royal Society of London A*, Vol. 277, No. 1371, Feb. 1964, pp. 468–497.
doi:10.1098/rspa.1964.0035

[4] Lawton, J., Mayo, P., and Weinberg, F., "Electrical Control of Gas Flows in Combustion Processes," *Proceedings of the Royal Society of London A*, Vol. 303, No. 1474, March 1968, pp. 275–298.
doi:10.1098/rspa.1968.0051

[5] Marcum, S., and Ganguly, B., "Electric-Field-Induced Flame Speed Modification," *Combustion and Flame*, Vol. 143, Nos. 1–2, Oct. 2005, pp. 27–36.
doi:10.1016/j.combustflame.2005.04.008

[6] Wisman, D., Marcum, S., and Ganguly, B., "Electrical Control of the Thermodiffusive Instability in Premixed Propane-Air Flames," *Combustion and Flame*, Vol. 151, No. 4, Dec. 2007, pp. 639–648.
doi:10.1016/j.combustflame.2007.06.021

[7] Williams, F., *Combustion Theory*, 2nd ed., Addison Wesley, Reading, MA, 1985, pp. 341–365.

[8] Kadowaki, S., "Body-Force Effect on the Lateral Movement of Cellular Flames at Low Lewis Numbers," *Physical Review E (Statistical Physics, Plasmas, Fluids, and Related Interdisciplinary Topics)*, Vol. 63, No. 2, 2001, pp. 026303.
doi:10.1103/PhysRevE.63.026303

[9] Sivashinsky, G., "Instabilities, Pattern Formation, and Turbulence in Flames," *Annual Review of Fluid Mechanics*, Vol. 15, Jan. 1983, pp. 179–199.
doi:10.1146/annurev.fl.15.010183.001143

[10] Kadowaki, S., "The Effects of Heat Loss on the Burning Velocity of Cellular Premixed Flames Generated by Hydrodynamic and Diffusive-Thermal Instabilities," *Combustion and Flame*, Vol. 143, No. 3, Nov. 2005, pp. 174–182.
doi:10.1016/j.combustflame.2005.05.012

[11] Darrieus, G., "Propagation d'un Front de Flame," communication presented at La Technique Moderne, 1938.

[12] Landau, L., "On the Theory of Slow Combustion," *Acta Physicochimica URSS*, Vol. 19, No. 1, 1944, pp. 77–85.

[13] Clanet, C., and Searby, G., "First Experimental Study of the Darrieus-Landau Instability," *Physical Review Letters*, Vol. 80, No. 17, 1998, pp. 3867–3870.
doi:10.1103/PhysRevLett.80.3867

[14] MacLatchy, C., "Langmuir Probe Measurements of Ion Density in an Atmospheric-Pressure Air-Propane Flame," *Combustion and Flame*, Vol. 36, 1979, pp. 171–178.
doi:10.1016/0010-2180(79)90057-9

[15] Boeuf, J., and Pitchford, L., "Electrohydrodynamic Force and Aerodynamic Flow Acceleration in Surface Dielectric Barrier Discharge," *Journal of Applied Physics*, Vol. 97, No. 10, May 2005, pp. 103307-1–103307-10.
doi:10.1063/1.1901841

[16] Raizer, Y., *Gas Discharge Physics*, Springer–Verlag, New York, 1997, p. 434.

[17] Starikovskii, A., Skoblin, M., and Hammer, M., "Influence of Weak Electric Fields on Flame Structure," AIAA Paper 2008-995, 2008.

[18] Goodings, J., Bhome, D., and Ng, C., "Detailed Ion Chemistry in Methane-Oxygen Flames. I. Positive Ions," *Combustion and Flame*, Vol. 36, 1979, pp. 27–43.
doi:10.1016/0010-2180(79)90044-0

[19] Pedersen, T., and Brown, R., "Simulation of Electric Field Effects in Premixed Methane Flames," *Combustion and Flame*, Vol. 94, No. 4, Sept. 1993, pp. 433–448.
doi:10.1016/0010-2180(93)90125-M

[20] Rodrigues, J., Agneray, A., Jaffrezic, X., Bellenoue, M., Labuda, S., Leys, C., Chernukho, A., Migoun, A., Cenian, A., Savel'ev, A., Titova, N., and Starik, A., "Evolution of Charged Species in Propane/Air Flames: Mass-Spectrometric Analysis and Modelling," *Plasma Sources, Science and Technology*, Vol. 16, No. 1, Feb. 2007, pp. 161–172.
doi:10.1088/0963-0252/16/1/021

[21] Riemann, K., "The Bohm Criterion and Sheath Formation," *Journal of Physics D: Applied Physics*, Vol. 24, No. 4, April 1991, pp. 493–518.
doi:10.1088/0022-3727/24/4/001

[22] Vejby-Christensen, L., Andersen, L., Heber, O., Kella, D., Pedersen, H., Schmidt, H., and Zajfman, D., "Complete Branching Ratios for the Dissociative Recombination of H_2O^+, H_3O^+ and CH_3^+," *Astrophysical Journal*, Vol. 483, July 1997, pp. 531–540.
doi:10.1086/304242

[23] Kojima, J., Ikeda, Y., and Nakajima, T., "Basic Aspects of OH(A), CH(A), and $C_2(d)$ Chemiluminescence in the Reaction Zone of Laminar Methane-Air Premixed Flames," *Combustion and Flame*, Vol. 140, Nos. 1–2, Jan. 2005, pp. 34–45.
doi:10.1016/j.combustflame.2004.10.002

[24] Kojima, J., Ikeda, Y., and Nakajima, T., "Measuring Local OH^* to Analyze Flame Front Movement in a Turbulent Premixed Flame," AIAA Paper 1999-2784, 1999.

[25] Hardalupas, Y., and Orain, M., "Local Measurements of the Time-Dependent Heat Release Rate and Equivalence Ratio Using Chemiluminescent Emission from a Flame," *Combustion and Flame*, Vol. 139, No. 3, Nov. 2004, pp. 188–207.
doi:10.1016/j.combustflame.2004.08.003

[26] Lawn, C., "Distributions of Instantaneous Heat Release by the Cross-Correlation of Chemiluminescent Emissions," *Combustion and Flame*, Vol. 123, Nos. 1–2, Oct. 2000, pp. 227–240.
doi:10.1016/S0010-2180(00)00129-2

[27] Pearlman, H., "Excitability in High-Lewis Number Premixed Gas Combustion," *Combustion and Flame*, Vol. 109, No. 3, May 1997, pp. 382–398.
doi:10.1016/S0010-2180(96)00192-7

[28] Glassman, I., *Combustion*, Academic Press, New York, 1996, pp. 125–144.

[29] Chen, J., Echekki, T., and Kollmann, W., "The Mechanism of Two-Dimensional Pocket Formation in Lean Premixed Methane-Air Flames with Implications to Turbulent Combustion," *Combustion and Flame*, Vol. 116, Nos. 1–2, Jan. 1999, pp. 15–48.
doi:10.1016/S0010-2180(98)00026-1

[30] Katta, V., Meyer, T., Brown, M., Gord, J., and Roquemore, W., "Extinction Criterion for Unsteady Opposing-Jet Diffusion Flames," *Combustion and Flame*, Vol. 137, Nos. 1–2, April 2004, pp. 198–221.
doi:10.1016/j.combustflame.2004.02.004

[31] Yuan, J., Ju, Y., and Law, C., "Coupled Hydrodynamic and Diffusional-Thermal Instabilities in Flame Propagation at Subunity Lewis Numbers," *Physics of Fluids*, Vol. 17, July 2005, pp. 074106-1–10.

[32] Starikovskaia, S., "Plasma Assisted Ignition and Combustion," *Journal of Physics D: Applied Physics*, Vol. 39, No. 16, Aug. 2006, pp. R265–R299.
doi:10.1088/0022-3727/39/16/R01

[33] Vincent-Randonnier, A., Larigaldie, S., Magre, P., and Sabel'nikov, V., "Plasma Assisted Combustion: Effect of a Coaxial DBD on a Methane Diffusion Flame," *Plasma Sources, Science and Technology*, Vol. 16, No. 1, Feb. 2007, pp. 149–160.
doi:10.1088/0963-0252/16/1/020

[34] Criner, K., Cessou, A., Louiche, J., and Vervisch, P., "Stabilization of Turbulent Lifted Jet Flames Assisted by Pulsed High Voltage Discharge," *Combustion and Flame*, Vol. 144, Nos. 1–2, Jan. 2006, pp. 422–425.
doi:10.1016/j.combustflame.2005.09.010

C. Avedisian
Associate Editor